

# DEEP RESIDUAL LEARNING FOR RECOGNISING ADULTERATION IN PULSES VIA THERMAL IMAGING

S. RUCKMANI<sup>1</sup>, Dr. M. SANTHI<sup>2</sup>, B. DIVYA<sup>3</sup>

<sup>1</sup>PG Student, Department of ECE, Saranathan College of Engineering, Tiruchirappalli, India.

<sup>2</sup>Professor, Department of ECE, Saranathan College of Engineering, Tiruchirappalli, India.

<sup>3</sup>Assitant Professor, Department of ECE, Saranathan College of Engineering, Tiruchirappalli, India.

**Abstract** - Food is the most essential requirement for sustenance of human life and it is one of the basic necessities of life. For optimal health, we should consume pure, nourishing, and adulterant-free food. Adulteration is the malicious contamination of food products with inferior, less expensive, inedible, or hazardous ingredients. Food adulteration means adding harmful substances to food products to contaminate or adulterate it. Pulses are a significant part of Indian cuisine, serving as a staple food item. Pulses may be adulterated by accidental, commercial, or metallic components, which can be harmful to health, rendering them unsafe for consumption and posing health risks. In order to guarantee the safety and quality of food, it is necessary to analyse pulses for any potential adulteration. In this paper, we propose a method for determining adulteration in Dal (Lentils) using ResNet-50, a deep learning model based on CNN. For this work, thermal images of pure dal and adulterated dal were used to classify the adulterated and unadulterated samples. Experimental results show that the proposed system can achieve high accuracy in detecting adulteration in pulses. The proposed system is also fast and requires minimal human intervention, making it suitable for use in food quality control systems.

**Key Words:** Adulteration, Deep learning, Thermal Images, Convolutional Neural Network (CNN), Residual Network, Pulses, lentils.

## 1. INTRODUCTION

Agriculture is an essential part of the Indian economy. The total area under cultivation and the quantity of agricultural goods have expanded quickly due to advancements in farming technologies. Recent times have seen a notable rise in the importance of agricultural development as it has accelerated the country's economic expansion [20]. Food safety and quality are crucial for ensuring the well-being of individuals, as they have a significant impact on human health. When a food is safe, it is nutritious, nontoxic, and does not harm human health [18]. It's important to be aware that food can be contaminated by various types of adulterants. It is illegal to adulterate food, and it is considered adulterated when it does not adhere to the government's legal criteria. Food adulteration occurs when harmful substances are intentionally or unintentionally added to it, reducing its quality [16]. All over India, pulses are cultivated. Likewise, India is the world's largest producer and consumer of pulses [8]. Lentils provide a substantial amount of essential dietary minerals, dietary fiber, protein, and carbohydrates. The edible seeds of legume-family plants are known as pulses. Pulses have a wide range of

colors, sizes, and shapes, and they grow in pods. Pulses are nutritious, nourishing, and simple to use in recipes. Growing pulses improves sustainable agriculture since they consume less water, reduce greenhouse gas emissions, and improve soil quality [4]. Sand, marble chips, stones, sludge, khesari dal or other pulses, metanil yellow, and soluble coal tar dye are used to adulterate pulses. These contaminants are deleterious to the well-being of humans [7]. Food products used in daily life that have been adulterated are hazardous and unhygienic to use.

**Table -1:** Food safety & standards for pulses as per act 2006, Rules 2011.

Type	Substances Added
Intentional Adulterants	Sand, marble chips, stones, mud, other fifth, Talc, Chalk powder, Water, mineral oil and harmful colour.
Incidental adulterants	Pesticide residues, droppings of rodents, larva in food.
Metallic Contaminants	Arsenic from pesticides, Lead from water, effluent from chemical industries, tin from Cans,

The above Table 1 shows the types of adulterants Food safety & Standards for pulses as per act 2006, Rules 2011. Before delivering the product to the consumer, it is highly important to check for adulteration of the pulses. Currently, agricultural products are categorized by humans based on their visual traits. Human visual examination is suboptimal because it is influenced by outside influences, including prejudice and restlessness, among others. To overcome these kinds of errors, we propose a Deep Learning model to detect adulteration in pulses. The proposed system uses ResNet-50, a deep residual learning for object identification and recognition and a skip connection option is available in this deep neural network. It will develop a rapid and accurate pulse adulteration-detecting technology.

## 2. RELATED WORKS

This study [1], Thermally treating rice samples, either in grain or flour form, with non-destructive and portable measuring equipment, such as a thermographic camera, makes it possible to collect a significant number of images of the cooling process from which differentiating characteristics between the varieties tested in this work can be inferred. The structural and water solubility variations of various amylose and amylopectin compositions are the main causes of the discrepancies in the thermographic pictures obtained during the cooling process of various rice samples. Classifying various types of rice and detecting probable adulterations with

an accuracy of more than 98% is possible using cognitive modeling and thermographic analysis.

In this paper [2], A thermographic camera was used to track the cooling of several samples of pure and contaminated honey (including varying percentages of rice syrup). Convolutional neural network (CNN) - based deep learning techniques were used on the generated images to function as both qualitative and quantitative adulteration detectors. The experimental component makes it more difficult to process the data. However, this is exactly the benefit of the tool, as once the mathematical model is created and optimized to meet its application, it doesn't need a lot of processing power to be used in practice. The end result was an algorithm with accuracy levels of 95% and 93% for measuring rice syrup and recognizing adulterated honey from various floral origins.

In system [3], The analysis of the thermal evolution of pure and contaminated extra virgin olive oil (EVOO) samples via deep learning has been the main focus of the application produced in this work. To detect and measure three different adulterations (refined olive oil, olive pomace oil, and sunflower oil) ranging from 0% to 8% in weight, mathematical models are used. This work suggests a novel approach that combines a thermographic technique with a contemporary alternative to mathematical modeling, such as CNNs. Convolutional neural networks perform statistically between 97 to 100% successfully in terms of classification.

This system [4] develops an approach for determining the quality of various grains, oil seeds, and pulses using deep learning, which is a CNN-based transfer learning methodology known as Dense Net. It estimates the grain quality based on the grayscale values of each pixel in the image. According to this study, image processing techniques are good at determining the grain quality.

It was examined whether it was possible to classify pulse flours (such as chickpea, yellow pea, navy bean, and green lentil) based on the type of pulse and milling techniques using hyperspectral imaging in the visible near infrared (Vis-NIR) (400-1000 nm) and shortwave infrared (SWIR) (1000-2500 nm). Unsupervised PCA and supervised PLS-DA were used to create both unsupervised and supervised classification models. However, as the chemical characteristics of the materials were related to the SWIR region, the milling process categorization was more precise when employing the SWIR range. The food sector can use hyperspectral imaging in the 400–2500 nm region along with multivariate data classification techniques to accurately characterize pulse flours with a 95% accuracy rate [5].

This research [6] develops a machine-learning-based food and formalin detection technique based on the Internet of Things. By applying machine learning algorithms including logistic regression, support vector machines, and K-NN classifiers to the experimental dataset, our system tracks the artificially added formalin as a preservative binary "1". The type of food was determined using conductive characteristics. Using a VOC HCHO gas sensor in combination with a Raspberry Pi, the system is capable of detecting formalin at a concentration of 1 to 50 ppm (parts per million). This system is a machine

learning-based dynamic and efficient method for food and formalin detection.

### 3. PROBLEM STATEMENT

When analyzing the caliber of agricultural products, the manual examination is inaccurate, inconsistent, and ineffective. After a specific period of time, it is human nature to get fatigued, exhausted, or lose focus. When widely utilized only for the identification of adulterants by color gradient methods, chromatography methods like gas chromatography and liquid chromatography are implemented [15]. These include the inspection, sorting, and authorization for identifying and evaluating the adulterants. Traditional approaches have the capacity to identify advanced techniques that are used even if their findings are not extremely precise and accurate. Modern techniques such as DNA testing, spectroscopy produce better results with accepted level of accuracy. These methods are time consuming, the equipment needed for analysis might be quite costly and for operating instruments, qualified or skilled individuals are needed.

To tackle these issues, this work proposes a ResNet-based Convolutional Neural Network (CNN) method to detect counterfeiting in pulses, and the thermal imaging concept is employed for dataset collection. ResNet increases the performance of deep neural networks by adding further neural layers while lowering the error rate. Thermal imaging is used to observe an object's internal temperature radiation. More than 98% accuracy is gained in this proposed work.

### 4. PROPOSED SYSTEM

Lentils, especially split pigeon pea (Arhar dal), also known as Toor dal, are the main emphasis of the suggested system. Thermal images of pure dal, khesari dal, adulterated dal (arhar dal with unwanted components like stones, sand particles and arhar dal with Khesari dal) are captured and it serves as a dataset for developing, evaluating, and verifying the model. The strategies employed and the image processing algorithm implemented are briefly detailed below. The digital images of Khesari dal, Split Pigeon Pea (Arhar dal), Arhar dal adulterated with Khesari dal, Arhar dal adulterated with stones and unwanted components are shown in fig.1.



Fig -1: Digital Images of Lentils

Lentils, beans, chick peas, and yellow peas are examples of pulses, which are annual leguminous crops. These crops are protein-rich foods, antioxidants, and fiber while being low in cholesterol and vitality, all of which contribute to a reduced

risk of CVD and Type 2 Diabetes mellitus. They are the primary nutritional source of Vitamin D in vegetarians' diets.

**Table -2: Effects of Adulterants**

Sl. No	Adulterant	Purpose of adding the Adulterants	Diseases or Health Effects
1	Sand, stones, husk, straws	For financial gains	Affect the digestive tract
2	Khesari dal	For financial gains	Crippling spastic paraplegia paralysis of the limbs

The reason for including the adulterants and its health effects is discussed above in Table 2. Khesari dal (*Lathyrus sativus*) pulse is a low-cost legume that does not require much irrigation. It is a staple food for many low-income people in Central India. Consuming Khesari dal as a staple food without a diverse diet can lead to an unbalanced diet. A diet based primarily on Khesari dal may lack the variety of nutrients necessary for maintaining good health. The risk of lathyrism (spastic paralysis of lower limbs) is particularly high when Khesari dal is consumed as a major portion of the diet, especially during times of food scarcity or famine. In some countries, there are regulatory restrictions on the sale and distribution of Khesari dal due to the associated health risks. This can limit its availability in the market. In some cases, Khesari dal is also used as animal feed. While this can be a way to utilize the crop, it can divert it from human consumption, potentially impacting food availability.

**4.1 CONCEPT OF THERMAL IMAGING**

Infrared radiation is used in thermal imaging technology, commonly referred to as infrared thermography, to record and analyze temperature fluctuations in scenes and objects. Direct visual perception of infrared radiation is impossible. Theoretically, all objects emit infrared radiation, the intensity of which is directly proportional to the temperature of the object. When compared to cooler objects, warmer ones emit more infrared radiation. As a result, infrared thermal imaging is finding extensive use in a number of sectors. It can be used in any application where temperature differences are necessary to support an identification, assessment, or examination of the product or activity. The capabilities of thermal imaging systems for automatic object recognition and anomaly detection have been improved via integration with other technologies like artificial intelligence and machine learning. Thermal imaging is a versatile and vital technology that is constantly developing and discovering innovative applications across many different sectors. The thermal images of khesari dal, Split Pigeon Pea (Arhar dal), Arhar dal adulterated with khesari dal, Arhar dal adulterated with stones and unwanted components are shown in fig.2.

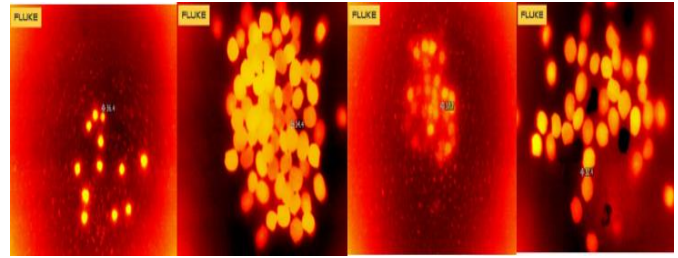


**Fig -2: Thermal Images of Lentils**

A thermal camera, also referred to as an infrared camera or a thermographic camera, is a tool that uses infrared light to generate images of objects and surfaces in its range of view depending on the temperature differences between them. In contrast to visible light cameras, which record the light that can be seen by our eyes, thermal cameras pick up on heat emissions from objects and translate them into visible images. Thermal camera works on the principle of detecting the infrared radiation emitted by objects. When this radiation is taken up by the camera's sensor, an image is produced with each pixel representing a different temperature. Real-time temperature differences can be measured and shown via thermal cameras. They are therefore suitable for a variety of applications.

The below fig.3 and fig. 4 represents some samples of the thermal images of arhar dal in the temperature state of heating and cooling process.

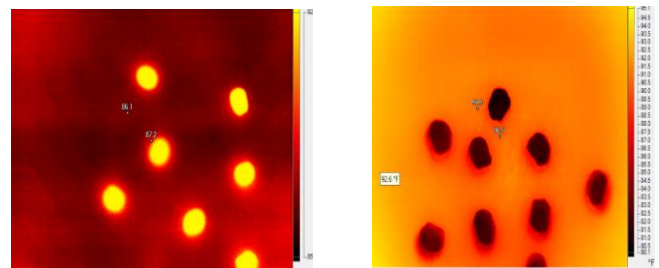


**Fig -3: Arhar dal in heat state Fig -4: Arhar dal in cool state**

Characteristics of thermal images: IR radiation is a form of electromagnetic radiation that is longer than visible light (400 to 750 nm) but shorter than microwaves (above 1 mm) in the electromagnetic spectrum. Typically, the wavelengths of infrared radiation range from about 750 nm to 1 mm. Due to their longer wavelengths than visible light, infrared waves can travel across crowded areas of gas and dust in space without being significantly scattered or absorbed. Since human eyes are only sensitive to the visible light spectrum, infrared radiation cannot be viewed by humans. an infrared wave is said to be a transverse wave and have the properties of absorption, reflection, refraction and interference. Infrared radiation's absorptivity, emissivity, transmissivity, and reflectivity differ depending on objects and materials.

The temperature of a body that absorbs all radiation that strikes its surface is how the Stephan-Boltzmann Law characterizes the power radiated by that body. The following formula can be used to express the radiation energy emitted by a black body per unit time, which is proportional to the

absolute temperature to the fourth power. Power radiated is defined by,

$$P = \epsilon \sigma T^4 A \text{ Watts}$$

Where P: Radiation energy/power

$\sigma$ : Stefan-Boltzmann Constant

T: Absolute temperature in Kelvin

$\epsilon$ : Emissivity of the material

A: Area of the emitting body

When using a thermal camera, infrared detectors measure radiation coming from an object's surface in the spectral range of 35 m (short wave) or 8–12 m (long wave).

#### 4.2 HARDWARE SETUP



Fig -5: Equipment setup of Thermal camera

The above fig.5 shows the setup of thermal camera. There are many models of thermal camera which includes industrial thermal camera, infrared radiometric thermal camera, professional and universal cameras, handheld cameras etc. When purchasing a thermal camera, the two most important considerations are the detector resolution and thermal sensitivity.

The Thermal Image Capturer, Laptop MSI RAIDER GE77 and the insulated chamber in which the food products to be validated are placed make up the hardware portion of the system. The setup is briefly described here. The laptop receives the images from the camera and processes them for further classification and analysis. The entire procedure is quite easy to complete and only requires a fundamental understanding of how to use a thermal imaging camera. The below fig.6 indicates that the camera is pointed at the insulated chamber.



Fig -6: Proposed hardware setup

The steps for capturing thermal images are as follows:

- A small aperture on top of a wooden insulation chamber with the following measurements: 30 cm x 30 cm x 25 cm is built for the thermal camera.
- The box is properly insulated to prevent heat transfer between the chamber and its surroundings.
- The food products (lentils) are positioned within the chamber in the desired areas, and the picture is then taken.
- To identify the presence of adulterants in food products, the collected images are subsequently supplied to the Resnet model.
- If there is a adulterant in the food product (lentils), the system then indicates it.

Wood, a good heat insulator, is used to construct the Insulation Chamber, preventing thermal radiation from the environment from interfering with the image. It has the following measurements: 30 cm long, 30 cm wide, and 25 cm high. Polystyrene (thermocol) is used to further cushion the inner layer in order to prevent heat from the chamber from escaping into the outside air. Then, a coating of black paint is applied to the surface so that the clean background provided by the black color allows for the viewing of the taken image in its highest quality. The photographs have an even higher quality thanks to the effective thermal absorption of this black paint layer. The fig.7 mentioned above shows the inner and outer structure of the insulation chamber.



Fig -7: Structure of Insulation chamber

Thermal cameras are adaptable technological tools that increase productivity and safety. Infrared energy is used by thermal imaging cameras to produce thermal images. The infrared energy is focused by the camera's lens onto a group of detectors, which then produce an elaborate thermogram pattern. To produce a thermal image that we can see and understand, the thermogram is then transformed into electrical impulses. A conventional thermal camera shows warmer objects as a yellow-orange hue that brightens as you proceed toward them and the object will take on a blue or purple hue as it becomes colder.

A portable camera equipped with an image processing system—typically provided by the manufacturer - that can record both RGB and thermal pictures serves as the basis of the thermography equipment. Its benefits include the lack of a need for fiber optics or a diode array detector during operation, as well as the equipment's inexpensive cost and ease of use when compared to hyperspectral imaging. Thermal imaging cameras usually have a spectral range in the far-infrared range between 7.5  $\mu\text{m}$  and 13  $\mu\text{m}$ , produce images of

320 × 240 pixels to 1280x960 pixels and provide high accuracy temperature measurements (up to 1200 °C).

The camera used in this work is the Fluke Thermal Camera, model TiX580 which is a high-performance thermal imaging camera made by Fluke Corporation. The TiX580 is well-known for its outstanding thermal resolution, which produces clear and in-depth thermal images. The thermal resolution, which is typically 640 x 480 pixels, is seen to be excellent for a variety of applications. It boasts a temperature range of up to 1832°F (1000°C) and features a touchscreen that can tilt 240°. The touchscreen interface of the TiX580 might be convenient to use, making it simple to explore menus, modify settings, and examine thermal photos on the camera's display. It likely supports various connectivity options, such as Wi-Fi or Bluetooth, allowing you to transfer images and data to a computer or mobile device for analysis and reporting. Tools for measuring temperature analysis may be integrated into the camera, such as temperature profiles, spot temperature measurement, and more. It has a long-lasting battery life and useful for wide range of applications. The fig.8 mentioned below represents the Fluke Thermal Camera TiX580.



Fig -8: Fluke Thermal Camera TiX580

### 4.3 SOFTWARE SETUP

The software elements of this work includes SmartView® Software and MATLAB libraries to create the Resnet-50 algorithm. A huge dataset can be created from a limited number of images by viewing, analyzing, and editing the images using the SmartView® Software. For the Neural Network to be analyzed, this dataset is then split into training, testing, and validation data. Users of SmartView can produce interactive reports, connect to numerous data sources, and carry out data analysis and visualization tasks. The below fig.9 shows the page of SmartView Software.



Fig -9: SmartView Software page

### 4.4 AN OVERVIEW OF CNN

Deep learning is a branch of machine learning and artificial intelligence (AI) that focuses on enabling artificial neural networks to carry out tasks that generally call for human-like intellect. Deep learning approaches have become quite popular and have produced cutting-edge achievements in a number of fields, including computer vision, natural language processing, speech recognition, and reinforcement learning. The basic steps of deep learning technique are shown in fig. 10.



Fig -10: Basic process of Deep Learning model

CNNs are specialized neural networks created for computer vision tasks. They are made up of convolutional layers, pooling layers, and fully connected layers. In applications like image classification, object identification, and image segmentation, CNNs have proved quite successful. It is a unique kind of deep neural network created primarily for processing and analyzing visual data, such as pictures and videos. They are modelled after the human visual system and perform tasks where the spatial relationships between data elements are crucial. The below fig.11 represents the architecture layer of CNN.

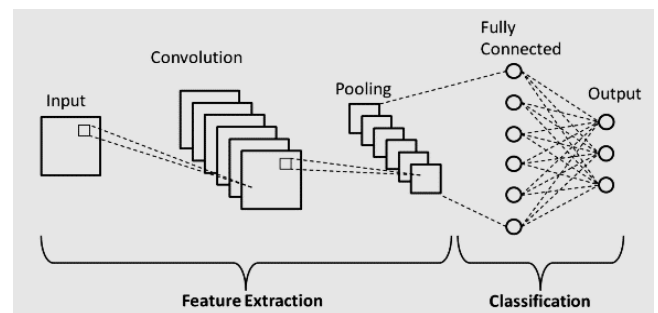


Fig -11: CNN Architecture

**Convolutional Layers:** Learnable filters (also known as kernels) are used by CNNs to scan the input data using convolutional layers. These filters move through the input, multiplying each element separately, then adding the results to create feature maps. Local patterns and features found in the input data are captured by convolutional layers. The fig.12 mentioned below indicates that the convolution operation has been implemented on a 5 X 5 input and a 3 X 3 filter.

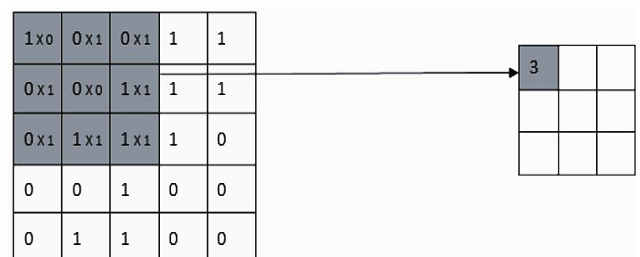


Fig -12: Process of Convolutional layer

**Pooling Layers:** Pooling layers, such as max-pooling or average-pooling, are used to shrink the feature maps' spatial dimensions while preserving crucial data. By pooling, the network becomes more resistant to changes in the input. The below fig.13 shows how max pooling is performed in CNN technique.

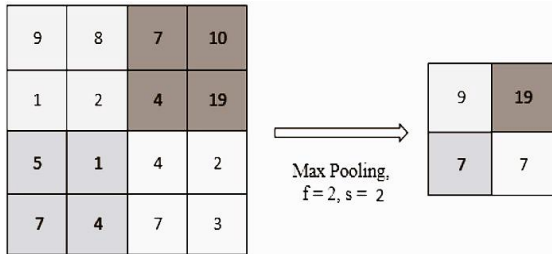


Fig -13: Steps of Max Pooling layer

**Activation function:** After convolution and pooling layers, non-linear activation functions like ReLU (Rectified Linear Unit) are used for the feature maps. These give the model non-linearity, allowing it to pick up complicated patterns.

**Fully Connected Layers (FCLs):** Following a number of convolutional and pooling layers, CNNs frequently include one or more FCLs. For final classification or regression, these layers flatten the output of earlier layers and feed it into a conventional feedforward neural network.

**Dropout:** A regularization method used in CNNs to avoid overfitting is called dropout. During training, it randomly sets a portion of the neurons' outputs to 0, which enhances generalization.

**Batch normalization** is another method for accelerating training and enhancing the stability of CNNs. Each layer's activations are normalized to have a zero mean and a unit variance.

**Strides:** To regulate how much the filter moves when scanning the input, convolutional layers might employ strides. Smaller feature maps are produced by a higher stride value.

**Padding:** Before convolution, padding can be applied to the input to regulate the feature maps' spatial dimensions. "Same" padding keeps the spatial dimensions, while "valid" padding means no padding is added, resulting in smaller feature maps.

Typically, CNNs are built in a hierarchical fashion, with a number of convolutional and pooling layers, to extract progressively complex, and sophisticated characteristics from the input data. Based on the specific work and dataset, the network's architecture may change.

A major issue with convolutional neural networks is the "Vanishing Gradient Problem. There is hardly any change in weights during backpropagation, because the gradient's value drops substantially. ResNet is used as a solution for this since it makes use of the "Skip connection" feature.

#### 4.5 RESNET-50 APPROACH

ResNet-50 is a deep convolutional neural network architecture from the ResNet (Residual Network) family having 50 layers. ResNet, short for Residual Networks is a classic neural network used as a backbone for many computer vision tasks. Because of its remarkable performance and ability to train very deep networks without suffering from the vanishing gradient problem, ResNet-50 is frequently used for a variety of computer vision tasks such as image classification, object recognition, and image segmentation. The most significant innovation with ResNet was that it enabled us to train highly deep neural networks with 150+ layers. Here, the training process is monitored by evaluating performance on the validation set and using techniques like early stopping to prevent overfitting. After training, evaluate the model's performance on the test dataset to assess its generalization ability. The fig.14 represents the working flow diagram of proposed system.

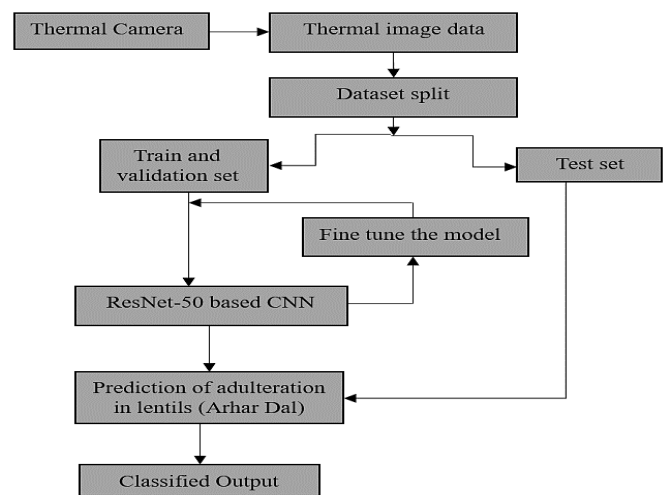


Fig -14: Flow Diagram of Proposed Work

The Procedure for the implemented work: We captured the thermal image datasets for Split Pigeon Peas (Arhar Dal), Khesari Dal, Adulterated Arhar Dal (with stones and Khesari Dal) by using thermal camera Fluke TiX580. Then the images are loaded into the database of the MATLAB. With the use of appropriate toolbox in MATLAB (R2019a), training and validation, and testing phases of ResNet-50 model are completed and achieved maximum accuracy level for the detection of adulteration in arhar dal.

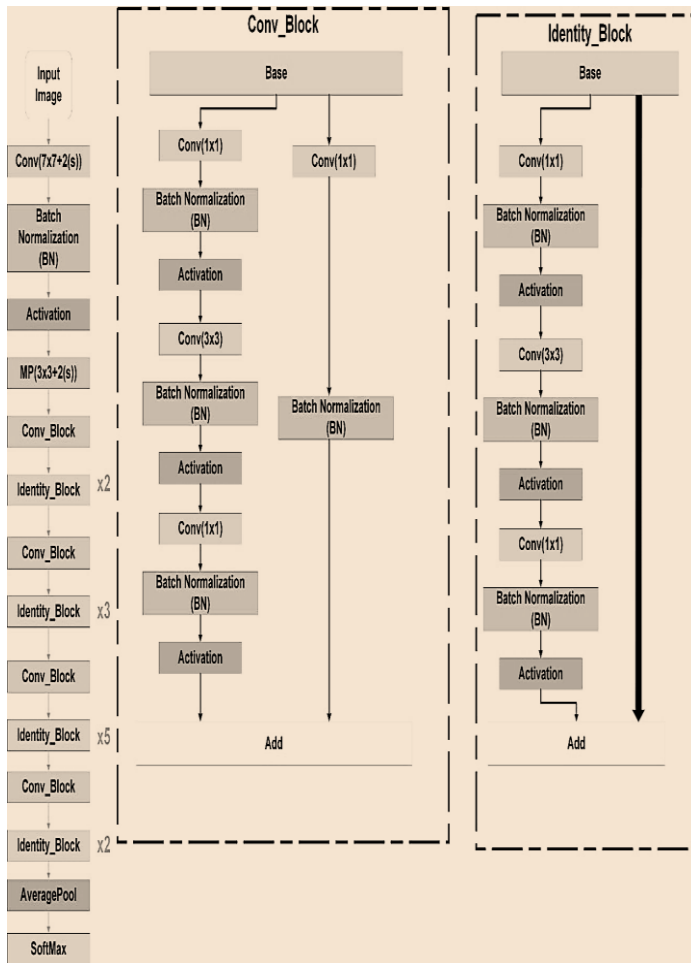


Fig -15: ResNet-50 Architecture

Residual networks, also known as ResNet50, are a ResNet model version having 48 Convolution layers, 1 MaxPool layer, and 1 Average Pool layer. ResNet is constructed from residual blocks, as shown in fig.15, by stacking residual blocks together, and each residual block has two 3x3 convolution layers. We doubled the number of filters on a regular basis and downsampled with stride 2. The ResNet lacks completely linked layers to output the 1000 classes.

Consider a neural network block with the input  $x$  and the goal of learning the true distribution  $H(x)$ . Let us refer to the difference (or residual) as

$$R(x) = \text{Output} - \text{Input} = H(x) - x$$

We acquire the below equation after rearranging  $R(x)$  equation,

$$H(x) = R(x) + x$$

The residual block is attempting to determine the true output,  $H(x)$ . Taking a closer look at the figure above, we can see that because  $x$  is causing an identity link, the layers are learning the residual,  $R(x)$ . A typical network's layers learn the real output ( $H(x)$ ), but a residual network's layers learn the residual ( $R(x)$ ). It has also been discovered that learning the residual of the output and input is easier than learning the residual of the input alone. As a result, because they are skipped and add no complexity to the design, the identity residual model allows for the reuse of activation functions from earlier levels.

The goal of ResNet is to locate the 'shortcut that links to the furthest layer,' as shown in below Fig. 16. Skipping numerous layers has little effect on total performance. Instead, the layers that were skipped are those with identical weights and the same prediction value. When this logic is used, stacking extra layers does not harm network performance, and mapping between residual levels is easier than fitting them straight into underlay mapping. Mathematically, it can be expressed as:  $\text{Output} = F(\text{Input}) + \text{Input}$  (i.e.)  $F(X) + x$ .

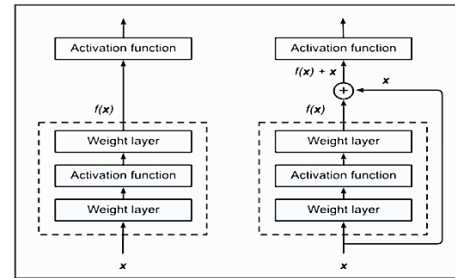


Fig -16: Skip Connection

There are two types of blocks in ResNet-50 that is Identity Block and Convolutional Block as shown in fig.17 and fig.18 respectively. If and only if 'input size==output size', the value 'x' is added to the output layer. If this is not the case, we append a 'convolutional block' to the shortcut path to make the input size equal to the output size.

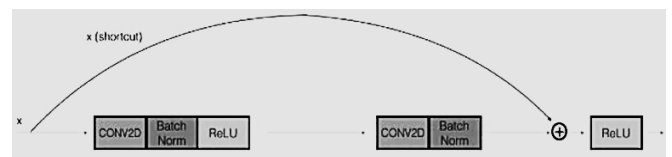


Fig -17: Identity Block

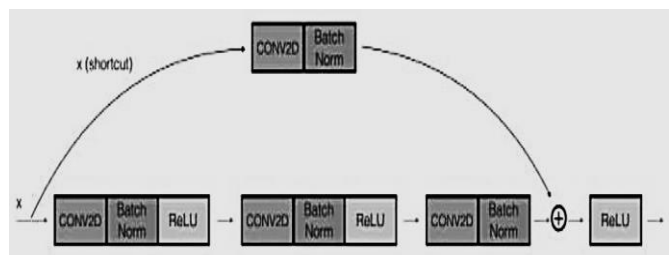


Fig -18: Convolutional Block

There are two methods for making the input size equal to the output size. They are Padding the input volume and Performing 1\*1 convolutions. Size of output layer is calculated using the expression:  $\lceil \frac{(n+2p-f)}{s} \rceil + 1$  where n= input image size, p=padding, s=stride, f=number of filters. For, 1\*1 convolutional layer, size of output layer =  $(n/2) * (n/2)$ , given the input size is 'n'. Pooling is used in CNNs to minimize image size. Instead, we use stride=2 here.

The input to a residual block is passed through a series of convolutional layers, batch normalization, and activation functions. This sub-path is responsible for learning the residual information. The residual mapping represents the difference between the desired output and the input. It is typically computed as the output of additional convolutional layers. These layers aim to capture the "residual" information that should be added to the input to obtain the desired output. The original input (or a projection of it) is added (element-wise) to the residual mapping. This skip connection bypasses the convolutional layers responsible for learning the residual. This addition operation is performed before applying an activation function. After the addition of the skip connection, an activation function (usually ReLU) is applied to the combined output. This ensures that the output remains non-linear.

ResNet-50 is a powerful and versatile deep learning architecture that excels in various computer vision tasks, offering benefits such as high accuracy, Effective Mitigation of Vanishing Gradient, Transfer Learning, Adaptable to Various Tasks, Interpretability, efficient training, and robust feature extraction. Its deep architecture and skip connections have made it a foundational model in the field of deep learning for image-related tasks.

## 5. IMPLEMENTATION OUTCOMES AND REVIEWS

### 5.1 Dataset

When a dataset is examined, it is divided into different phases and the performance of the dataset and classifier is assessed by how well they recognize objects [12]. The suggested Residual Network model (ResNet50) is trained, validated and tested using images (around 500) acquired from a thermal camera classified with four different classes, and encompassing two different types of dal and unintentional particles. The complete image database has been randomly divided into following groups: 400 images for Training and Validation phases, 100 images for Testing phase.

### 5.2 Training and Validation

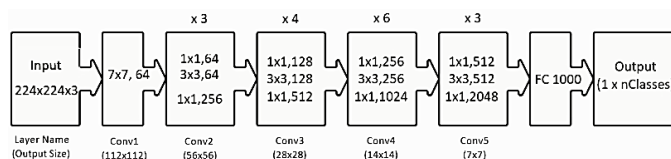


Fig -19: Residual Network-50

The above fig.19 shows the flow of residual network-50 which has depicted residual units, filter size, and convolutional layer outputs. In the convolutional layer block, the notation kxk, n specifies a filter of size k and n channels. The completely connected layer with 1000 neurons is denoted by FC 1000. The repetition of each unit is represented by the number at the top of the convolutional layer block. The number of n Classes denotes the number of output classes.

The model is first trained using visuals from the train set. The trained model is then validated and used to perform classification on the test set images. The below Fig. 20 depicts the accuracy and variance of loss during training and validation phases with regard to the number of epochs processed.

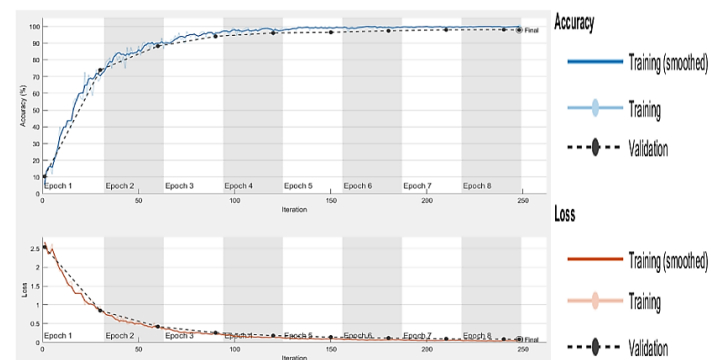


Fig -20: Accuracy & loss of training and validation subsets in terms of the number of epochs

### 5.3 Testing

The below fig.21 and fig.22 shows the results obtained during testing phase of the proposed work. Here the classification of 4 different labels have been achieved perfectly with accuracy (success rate) of more than 98%.

### 5.4 Performance Evaluation

We took the counts of cases for each round of cross-validation to compare these categorization attempts.

True Positives (TP): The number of correctly predicted positive samples.

True Negatives (TN): The number of correctly predicted negative samples.

False Positives (FP): The number of incorrectly predicted positive samples.

False Negatives (FN): The number of incorrectly predicted negative samples.

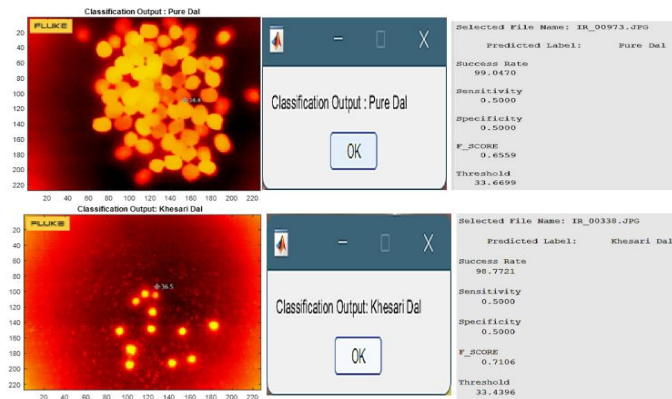


Fig -21: Results of testing phase

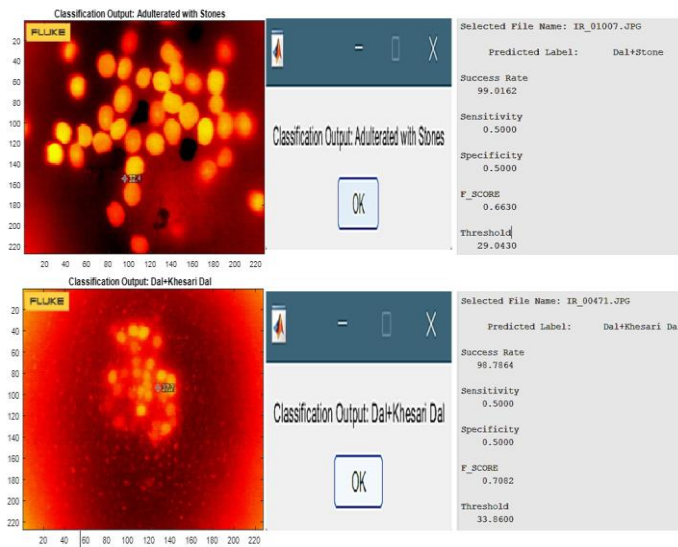


Fig -22: Results of testing phase

Accuracy, sensitivity, specificity, F-score are the computations used for the analysis of the outcomes. The following are the implications of those theorems:

- **Accuracy:** It measures the overall correctness of predictions. It is the ratio of the number of correct predictions to the total number of predictions.

$$\text{Accuracy} = \frac{TP + TN}{TP + TN + FP + FN}$$

- **Sensitivity / Recall / True Positive Rate:** Sensitivity measures the ability of the model to correctly identify positive samples.

$$\text{Sensitivity} = \frac{TP}{TP + FN}$$

- **Specificity:** Specificity measures the ability of the model to correctly identify negative samples.

$$\text{Specificity} = \frac{TN}{TN + FP}$$

- **F-score (F1-score):** The F-score is the harmonic mean of precision and recall and provides a balance between precision and recall. It's often used when the class distribution is imbalanced.

$$\text{F-Score} = 2 * \frac{\text{Precision} * \text{Recall}}{\text{Precision} + \text{Recall}}$$

- **Precision:** The ratio of correctly predicted positive instances (TP) to the total number of instances predicted as positive (TP + FP).

$$\text{Precision} = \frac{TP}{TP + FP}$$

These metrics evaluate the performance of ResNet model. Calculate the values of TP, TN, FP, and FN from the model's predictions and the ground truth labels for our dataset to use these formulas effectively.

## 6. CONCLUSION

Adulteration of pulses with contaminants is a major issue in the food sector, and reliable and efficient methods for recognizing such adulteration are essential. The ResNet-50-based CNN model is an effective tool for identifying adulteration in lentils with a high degree of precision. The success rate of the model for detecting adulteration in lentils depends on the quality of the dataset used for training. A well-labelled dataset that contains images of different types can help to improve the precision of the model. ResNet-50's deep learning capabilities have improved the accuracy (more than 98%) of object recognition and classification within thermal images. It also employs skip linking to add the output of a prior layer to a subsequent layer and this alleviates the fading gradient difficulties. Thermal cameras used in this study helps to detect objects based on their heat signatures, which can be valuable in low-light or adverse weather conditions. Thus, thermal imaging provides additional information compared to visible light cameras, especially in scenarios where visibility is limited due to smoke, fog, or darkness. The suggested system can be used in food processing plants and laboratories to ensure the quality and safety of the lentils. This study helps to shorten the time required, making it a viable choice for the food trade. In future, this study can be enhanced by exploring deeper architectures to improve performance by developing more efficient versions of ResNet that maintain or even improve accuracy while reducing computational and memory requirements. Models like ResNet-101, ResNet-152, and even deeper variants can be developed, which could offer better feature extraction and generalization. Combining multiple ResNet models or other architectures into an ensemble can often boost performance and improve model robustness.

## ACKNOWLEDGEMENT

The authors wish to acknowledge the All India Council for Technical Education (AICTE) for funding this project under the Research Promotion Scheme (RPS) [File No. 8-70/FDC/RPS/POLICY-1/2021-22].

## REFERENCES

- [1] Leidy V. Estrada, Sandra Pradana-Lopez, Ana M. P´erez-Calabuig, Mar´ıa Luz Mena, John C. Cancilla, Jos´e S. Torrecilla (Aug 2021), “Thermal imaging of rice grains and flours to design convolutional systems to ensure quality and safety” - Food Control, Vol. 121, 107572, ISSN 0956-7135, doi: 10.1016/j.foodcont.2020.107572.
- [2] Manuel Izquierdo, Miguel Lastra-Mej´ıas, Ester Gonz´alez-Flores, John C. Cancilla, Miriam P´erez, Jos´e S. Torrecilla, (Mar 2020), “Convolutional decoding of thermographic images to locate and quantify honey adulterations”, Talanta, Volume 209, 120500, ISSN 0039-9140, doi: <https://doi.org/10.1016/j.talanta.2019.120500>.
- [3] Manuel Izquierdo , Miguel Lastra-Mej´ıasa , Ester Gonz´alez-Flores , John C. Cancillab , Regina Aroca-Santosa, Jos´e S. Torrecilla (Feb 2020), “Deep thermal imaging to compute the adulteration state of extra virgin olive oil” - Computers and Electronics in Agriculture, Vol. 171, 105290, doi:10.1016/j.compag.2020.105290.
- [4] Vinatha Sree G, Tejaswini R, Nikhil Kalyan N, Venkata Sai Prasad G, Rasool Bash S K (Apr 2022), “Quick analysis of Quality of Cereals, Oil seeds and pulses using AI” – IOSR(JECE), Volume 17, Issue 2, pp. 53-56, doi: 10.9790/2834-1702015356.
- [5] Chitra Sivakumar, Muhammad Mudassir Arif Chaudhry, Jitendra Paliwal (Nov 2021), “Classification of pulse flours using near-infrared hyperspectral imaging” - LWT, Volume 154, 112799, ISSN 0023-6438, doi: <https://doi.org/10.1016/j.lwt.2021.112799>.
- [6] S. P. S. Brightly, G. S. Harini and N. Vishal, "Detection of Adulteration in Fruits Using Machine Learning," 2021 Sixth International Conference on Wireless Communications, Signal Processing and Networking (WiSPNET), Chennai, India, 2021, pp. 37-40, doi: 10.1109/WiSPNET51692.2021.9419402.
- [7] Sudheer B. V, Lakshmi Devi M.K, Krishna Rao D.V. (May 2015) - “Adulteration of the Pulses in Coastal Region of Andhra Pradesh”. Journal of Evolution of Medical and Dental Sciences, Vol. 4, Issue 36, PP. 6187-6192, doi: 10.14260/jemds/2015/902.
- [8] Jaspreet Kaur, Vijay Kumar Banga (March 2014), “Image Processing in Quality Assessment of Pulses” - IJCEM, Vol. 17 Issue 2, ISSN: 2230-7893.
- [9] M. O. Ramkumar, S. Sarah Catharin, V. Ramachandran, and A. Sakthikumar, “Cercospora Identification in Spinach Leaves Through Resnet-50 Based Image Processing,” J. Phys. Conf. Ser., vol. 1717, no. 1, p. 012046, Jan. 2021, doi: 10.1088/1742-6596/1717/1/012046.
- [10] V. Kumar, H. Arora, Harsh and J. Sisodia, "ResNet-based approach for Detection and Classification of Plant Leaf Diseases," 2020 International Conference on Electronics and Sustainable Communication Systems (ICESC), Coimbatore, India, 2020, pp. 495-502, doi: 10.1109/ICESC48915.2020.9155585.
- [11] Pitprecha, Nattapat & Mruetusatorn, Saprasit, “Apple-bruised detection using infrared thermal imaging analytical techniques”, (May 2020), Conference: TNIAC2020 at Thai-Nichi Institute of Technology, Bangkok, Thailand.
- [12] Merlne Magrina and M. Santhi, "Ancient Tamil Character Recognition from Epigraphical Inscriptions using Image Processing Techniques", Journal of Telecommunication Study, Vol. 4, Issue. 2, 2019.
- [13] Vitalis, Flora, John-Lewis Zinia Zaukuu, Zsanett Bodor, Balkis Aouadi, G´eza Hitka, Timea Kaszab, Viktoria Zsom-Muha, Zoltan Gillay, and Zoltan Kovacs, “Detection and Quantification of Tomato Paste Adulteration Using Conventional and Rapid Analytical Methods”, (Oct 2020), Sensors 20, no. 21: 6059. doi: <https://doi.org/10.3390/s20216059>.
- [14] K. He, X. Zhang, S. Ren and J. Sun, "Deep Residual Learning for Image Recognition," 2016 IEEE Conference on Computer Vision and Pattern Recognition (CVPR), Las Vegas, NV, USA, 2016, pp. 770-778, doi: 10.1109/CVPR.2016.90.
- [15] Aditya, Manuj.P, Rabiabasari Kagadagar, Dr. Anand Jatti, Dr. K.B.Ramesh, “Food Adulteration Detector using Image Processing and CNN”, (Jul 2023), International Journal of Emerging Technologies and Innovative Research ([www.jetir.org](http://www.jetir.org)), ISSN:2349-5162, Vol.10, Issue 7, page no. i367-i372, Available at: <http://www.jetir.org/papers/JETIR2307849.pdf>.
- [16] S. Hariprasath and M. Santhi, "Efficient Implementation of Multi Modal Biometric Pattern Recognition using Supervised Neural Network", International Journal of Advanced Technology in Engineering and Sciences, pp. 323-336, Vol. 5, Issue. 2, Feb 2017, ISSN: 2348-7550.
- [17] Awasthi, Shruti & Jain, Kirti & Das, Anvesha & Alam, Raza & Surti, Ganesh & N., Kishan, “Analysis of Food quality and Food Adulterants from Different Departmental & Local Grocery Stores by Qualitative Analysis for Food Safety,” (Mar-Apr. 2014), Department of Biochemistry, Garden City College, Bangalore. et al., IOSR J. Environ. Sci. Toxicol. Food Technol., vol. 8, no. 2, pp. 22–26, doi: 10.9790/2402-08232226.
- [18] Yong He, Xiulin Bai, Qinlin Xiao, Fei Liu, Lei Zhou & Chu Zhang, “Detection of adulteration in food based on nondestructive analysis techniques: a review”, (Jun 2020), Critical Reviews in Food Science and Nutrition, 61:14, 2351-2371, PMID: 32543218, doi: 10.1080/10408398.2020.1777526.
- [19] Vishwesh Nagamalla, Muthu Kumar B, Neha Janu, Anusha Preetham, Syam Machinathu Parambil Gangadharan, Mejdal A. Alqahtani and Rajnish Ratna (Jun 2022), “Detection of Adulteration in Food Using Recurrent Neural Network with Internet of Things” - Hindawi (Journal of Food Quality), Article ID: 6163649, 11 pages, doi: 10.1155/2022/6163649.
- [20] 3. B. Divya, M. Santhi, "Modified Convolutional Neural Network Based Automatic Detection and Classification Of Insects In Agricultural Fields", Journal Of Green Engineering (Jge), pp. 2766-2783, Vol. 11, Issue. 3, Mar 2021.
- [21] Ahmad Jahanbakhshi, Yousef Abbaspour-Gilandeh, Kobra Heidarbeigi, Mohammad Momeny, “Detection of fraud in ginger powder using an automatic sorting system based on image processing technique and deep learning”, (Sep 2021), 2021, Computers in Biology and Medicine, Volume 136, 104764, ISSN 0010-4825, doi: <https://doi.org/10.1016/j.combiomed.2021.104764>.
- [22] Manasha S, Janani M (April 2016), “Food adulteration and its problems (intentional, accidental and natural food adulteration)” - IJRFM Volume 6, Issue 4, (ISSN 2231-5985).
- [23] Lili Zhu, Petros Spachos, Erica Pensini, Konstantinos N. Plataniotis (Mar. 2021), “Deep learning and machine vision for food processing: A survey” - Current Research in Food Science, vol.4, pp. 233–249, ISSN 2665-9271, doi: 10.1016/j.crf.2021.03.009.